Available online at www.sciencedirect.com
ScienceDirect
Solid State Communications 141 (2007) 600–604
solid state communications
www.elsevier.com/locate/ssc

Optical properties of p-type ZnO doped by lithium and nitrogen

X.H. Wang[a,b], B. Yao[a,*], D.Z. Shen[a], Z.Z. Zhang[a], B.H. Li[a], Z.P. Wei[a,b], Y.M. Lu[a], D.X. Zhao[a], J.Y. Zhang[a], X.W. Fan[a], L.X. Guan[c], C.X. Cong[c]

[a] *Key Laboratory of Excited State Processes, Changchun Institute of Optics, Fine Mechanics and Physics, Chinese Academy of Sciences, Changchun, 130033, PR China*
[b] *Graduate School of Chinese Academy of Sciences, Beijing 100039, PR China*
[c] *Department of Physics, Jlin University, Changchun, 130023, PR China*

Received 5 September 2006; received in revised form 26 December 2006; accepted 3 January 2007 by R. Merlin
Available online 9 January 2007

Abstract

A lithium and nitrogen doped p-type ZnO (denoted as ZnO: (Li, N)) film was prepared by RF-magnetron sputtering and post annealing techniques with c-Al_2O_3 as substrate. Its transmittance was measured to be above 95%. Three dominant emission bands were observed at 3.311, 3.219 and 3.346 eV, respectively, in the 80 K photoluminescence (PL) spectrum of the p-type ZnO:(Li, N), and are attributed to radiative electron transition from conduction band to a Li_{Zn}–N complex acceptor level (eFA), radiative recombination of a donor–acceptor pair and recombination of the Li_{Zn}–N complex acceptor bound exciton, respectively, based on temperature-dependent and excitation intensity-dependent PL measurement results. The Li_{Zn}–N complex acceptor level was estimated to be about 126 meV above the valence band by fitting the eFA data obtained in the temperature-dependent PL spectra.

PACS: 71.55.Gs; 78.20.-e

Keywords: A. Thin films; D. Optical properties; D. p-Type; D. Semiconductor

1. Introduction

ZnO is a wide-bandgap (3.437 eV at 2 K) [1] semiconductor with a large exciton binding energy (60 meV), which allows the exciton luminescence at room temperature and makes ZnO become a promising material for optoelectronic devices, such as ultraviolet light-emitting diodes, laser diodes and photodetectors. It has been intensively investigated in the recent years. To realize ZnO-based photoelectric devices, the high quality p-type must be fabricated, but it seems to be very difficult.

In the present work, the fabrications of p-type ZnO were mainly doped by single acceptor, such as Li [2], N [3–5], P [6–9], As [10–12], Sb [13] or codoped by III–V elements, such as (Al, N) [14], (Ga, N) [15]. Among the single acceptor dopants, theoretically, Li substituting for Zn (Li_{Zn}) possesses the shallowest acceptor level [16]. However, the fabrication of p-type ZnO doped by Li is limited due to formation of donor complex, such as interstitial Li atom (Li_i) and Li_{Zn}–Li_i complex [17]. So, it is important to restrain formation of Li_i for realization of Li doped p-type ZnO. It may be an effective method of suppression of Li_i by codoping of Li and a dopant, which can bond with Li to form an acceptor complex with shallow level. N was used as such a dopant in our research work recently, and a p-type ZnO codoped by Li and N (denoted as p-type ZnO:(Li, N)) with good electrical properties was obtained by using RF-magnetron sputtering and annealing techniques [18]. Recently, the p-type ZnO:(Li, N) was also realized by pulsed laser deposition [19]. The p-type conduction of the ZnO:(Li, N) is attributed to formation of Li_{Zn}–N complex acceptor [18].

In the present work, the optical properties of the p-type ZnO:(Li, N) will be investigated, and the photoluminescence related to Li_{Zn}–N complex acceptor of the p-type ZnO:(Li, N) will be discussed in detail.

* Corresponding author.
E-mail address: binyao@jlu.edu.cn (B. Yao).

0038-1098/$ - see front matter © 2007 Elsevier Ltd. All rights reserved.
doi:10.1016/j.ssc.2007.01.002

2. Experimental procedures

A Zn–Li alloy with nominal 2 at.% Li was prepared by arc-melting technique. X-ray diffraction (XRD) confirmed that Li incorporated into Zn by substituting for Zn, and the Li content was estimated to be about 1.63 at.% by using the XRD data and Vegard formula. A 500 nm thick lithium and nitrogen doped ZnO film with wurtzite structure (denoted as ZnO:(Li, N)) was grown on a *c*-plane Al_2O_3 substrate at 300 K by RF-magnetron sputtering using the Zn–Li alloy as the target. A mixed gas of oxygen and nitrogen with a ratio of 1:1 was used as the sputtering gas with a total pressure of 1.0 Pa. Before deposition, the substrate was treated with ethanol in an ultrasonic bath to remove surface contamination and etched in hot (160 °C) H_2SO_4:H_3PO_4 (3:1) solution for 10 min and then rinsed in de-ionized water (18.2 MΩ cm) and blown dry using high-purity nitrogen. The as-grown films were divided into four pieces, three pieces of which were annealed in a N_2 flow for 30 min at 500, 600 and 700 °C respectively.

X-ray diffraction (XRD) measurements were performed by using a Rigaku O/max-RA X-ray diffractometer with Cu Kα radiation ($\lambda = 1.5418$ Å). Optical transmission and absorption spectra were carried out by using a UV-3101PC spectrometer. The temperature-dependent PL of the p-type ZnO:(Li, N) film was measured at temperatures ranging from 80 K up to 300 K by using the UV Labran Infinity Spectrophotometer made by the Jobin Yvon Company, which is excited by the 325 nm line of a He–Cd laser with a power of 50 mW.

3. Experimental results and discussion

The Hall measurement results show that the as-grown film behaved like an insulator, and the films annealed at 500 and 700 °C behaved with a weak p-type conduction, exhibiting alternative appearance of positive and negative Hall coefficient in the measurement process. A stable p-type conduction with hole concentration of 3.07×10^{16} cm^{-3} was realized by annealing the as-grown film at 600 °C. To understand the effects of the annealing on structure and band gap of the ZnO:(Li, N), measurements of XRD, transmission and absorption were carried out for the as-grown film and for the films annealed at 500, 600, 700 °C. Fig. 1(a)–(d) show XRD patterns of the as-grown film and annealed at 500, 600 and 700 °C respectively. The as-grown film only exhibits a weak and broad (002) diffraction peak, indicating that the film has preferential orientation in (002) direction and has poor crystal quality. Upon annealing, the (002) peak becomes strong and sharp, and the diffraction angle shifts towards the high angle direction, as shown in Fig. 1. The former implies improvement of crystal quality of the film, and the latter is due to relaxation of tensile stress in the film [20]. The lattice constant *c* of the as-grown and annealed films calculated by using data of the (002) diffraction peak was found to be 0.5262, and 0.5197 nm, respectively, which shows that the constant *c* of the as-grown film is larger than that of bulk ZnO of 0.5207 nm [21], indicating that the as-grown film has residual tensile strain along the *c*-axis and compressive biaxial strain within the growth plane [22].

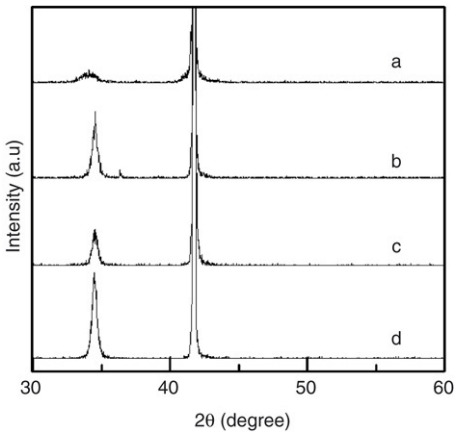

Fig. 1. XRD patterns of as-grown ZnO:(Li, N) film (a) and the films annealed at 500 (b), 600 (c) and 700 °C (d), respectively.

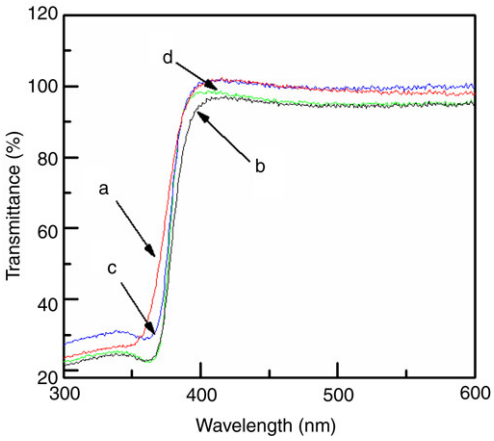

Fig. 2. Transmission spectra of as-grown ZnO:(Li, N) film (a) and the films annealed at 500 (b), 600 (c) and 700 °C (d), respectively.

After annealing, the lattice constant *c* decreases from 0.5262 to 0.5197 nm, indicating that the strain in the as-grown film is relaxed. The lattice constant *c* of the films annealed at 500, 600 and 700 °C is somewhat smaller than that of bulk ZnO, this is due to the fact that covalent bond length of Li–N (0.197 nm) is somewhat smaller than that of Zn–O (0.199 nm), and the incorporation of Li and N into ZnO in a form of Li–N will decrease the lattice constant *c*. As will be shown in Fig. 3, the relaxation of the compressive biaxial strain due to annealing can also be illustrated by the decrease of band gap.

The transmission spectra for the as-grown and annealed ZnO:(Li, N) are illustrated in Fig. 2. The transmittances of all films are over 95% in the visible region, which is higher than that of N-doped p-type ZnO [23], and the transmittance decreases sharply near absorption edge, implying high crystallinity of the p-type ZnO doped by lithium and nitrogen.

To determine the band gap of the film, we use the theory developed for optical transitions in insulators [24,25], where the absorption coefficient (α) of ZnO is a parabolic function of the incident energy and the optical band gap,

$$\alpha(h\nu) = A^*(h\nu - E_g)^{1/2}, \quad (1)$$

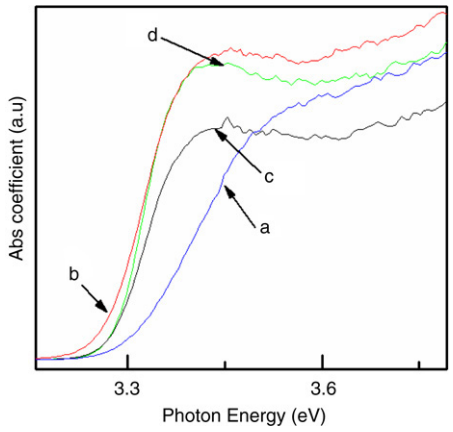

Fig. 3. Absorption spectra of as-grown ZnO:(Li, N) film (a) and the films annealed at 500 (b), 600 (c) and 700 °C (d) respectively.

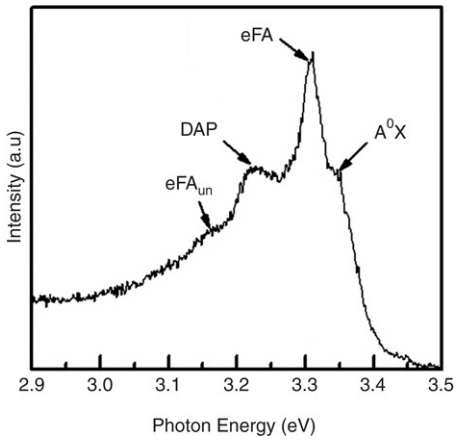

Fig. 4. 80 K PL spectra of the p-type ZnO:(Li, N) obtained at annealing temperature of 600 °C.

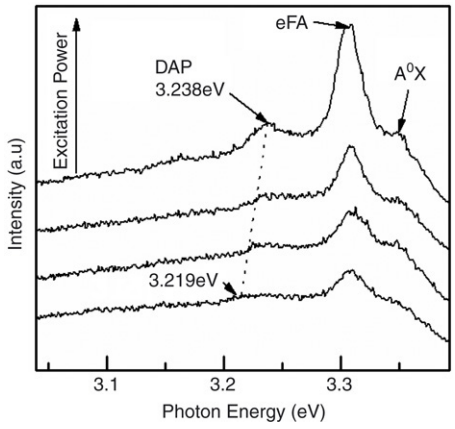

Fig. 5. 80 K excitation intensity-dependent PL spectra of the p-type ZnO:(Li, N) obtained at annealing temperature of 600 °C.

where A^* is a function of the refractive index of the material, the reduced mass, and the speed of light in vacuum, $h\nu$ is photon energy, E_g is band gap. Using this relationship, the band gaps of the films can be evaluated in the standard manner from a plot of α^2 as a function of the energy of the incident radiation and extrapolating the linear part of the curve to intercept the energy axis [26]. The variations of square absorption coefficient α^2 versus photon energy $h\nu$ in the fundamental adsorption region are plotted in Fig. 3. The band gaps of the as-grown film and those of the annealed one at 500, 600 and 700 °C are 3.292, 3.271, 3.269 and 3.272 eV, respectively. The band gap of the annealed film is obviously smaller than that of the as-grown. It is well known that the band gap of a semiconductor is affected by the residual strain in the film. A tensile strain results in a decrease in the band gap while a compressive strain causes an increase [27]. As discussed above, the decrease of band gap is due to the relaxation of the compressive biaxial strain after annealing.

Fig. 4 shows low-temperature (80 K) PL spectrum of the p-type ZnO:(Li, N) obtained at annealing temperature of 600 °C. The PL spectrum consists of three main emission bands, located at 3.311, 3.346 and 3.219 eV, respectively, and one weak broad band centered at 3.165 eV in the UV region. As will be shown later, the dominant peak positioned at 3.311 eV can be due to electronic radiative transition from conduction band to neutral acceptor level (eFA). The broad bands centered at 3.219 and 3.165 eV can be attributed to recombination of a donor–acceptor pair (DAP) and free electron to unidentified deep neutral acceptor level transition (eFA_{un}). The emission band centered at 3.346 eV is in the energy range (3.315–3.358 eV) of acceptor-bound exciton in N [5]-, P [7]- and As [10]-doped p-type ZnO reported previously, but it has hardly been observed in doped p-type ZnO reported up to now (it was reported in nominally undoped p-type ZnO on Si) [28], and it can be ascribed to a neutral acceptor-bound exciton emission (A^0X).

In order to investigate the origins of the emission bands, the excitation intensity-dependent PL and temperature-dependent PL measurements were performed, respectively. As we know, the energy of the DAP luminescence is represented as follows [29]:

$$E_{\mathrm{DAP}} = E_g - (E_D + E_A) + e^2/4\pi\varepsilon R_{DA} \tag{2}$$

where E_g, E_D, E_A, and e, ε are band gap energy, donor binding energy, acceptor binding energy, elementary electric charge and dielectric constant, respectively, R_{DA} is the distance between the involved donor and acceptor. When the excitation intensity is increased, the number of occupied donor and acceptor centers increases, resulting in decrease of their average distance R_{DA}, so that DAP luminescence peak shows a blue-shift. Fig. 5 shows excitation intensity-dependent PL spectra taken at 80 K. It indicates that the emission of the DAP shifts from 3.219 to 3.238 eV with increasing excitation intensity, which is consistent with the characteristics of DAP mentioned above, we assigned this emission band to the donor–acceptor pair luminescence.

Fig. 6 shows the temperature-dependent PL spectra, which shows that the 3.311 eV band reveals red shift with increasing temperature, while the 3.219 eV band shows distinctly blue shift first, and then gradually merges into the 3.311 eV band at about 150 K due to thermal ionization of donors of DAP [30], this is a typical characteristic of transition between radiative recombination of a donor–acceptor pair (DAP) and

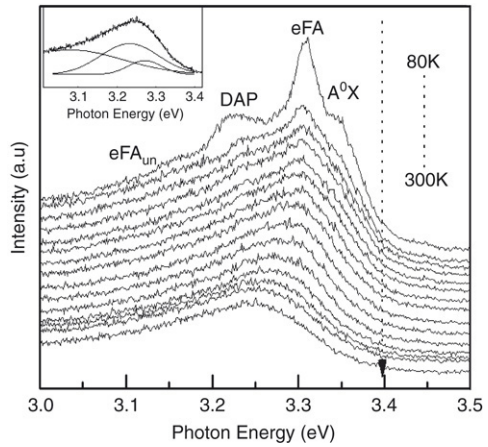

Fig. 6. Temperature-dependent PL spectra of the p-type ZnO:(Li, N) obtained at annealing temperature of 600 °C measured at temperatures from 80 K to 300 K. The spectra were vertically displaced for clarity, the inset is the room-temperature (RT) PL spectra by using the Gaussian fitting.

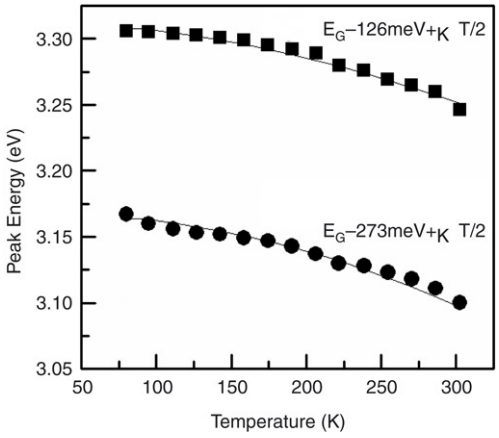

Fig. 7. Temperature-dependent photon energies of eFA (■) and eFA_{un} (•) indicated in Fig. 6. The solid lines represent the fitting to the data.

radiative electron transition from conduction band to acceptor (eFA) [29]. Therefore, the 3.311 eV band is ascribed to radiative electron transition from conduction band to a Li_{Zn}–N complex acceptor level (eFA). Similar results were also observed in the temperature-dependent PL spectra of p-type ZnO:Sb [31] and ZnO:Li [32].

The temperature dependence of the eFA band centered at 3.311 eV can be well described as the following:

$$E_{\mathrm{FA}}(T) = E_g(T) - E_A + \kappa T/2 \tag{3}$$

where $E_g(T)$ is the temperature-dependent band gap, and follows the Varshni-type equation [33], E_A, κ, and T are acceptor level, Boltzmann constant, and temperature, respectively. By fitting the energies of the eFA band at different temperatures with Eq. (3), as shown in Fig. 7, the Li_{Zn}–N complex acceptor level can be estimated to be about 126 meV.

The intensity of the emission band centered at 3.346 eV decreases very fast with increasing temperature, and it cannot be detected above 140 K. As shown in Fig. 7, the acceptor level (E_A) is about 126 meV above the valence band. Using the Haynes rule $E_b^{A^0X}/E_A \approx 0.1$ for ZnO material system [34], where E^{A^0X} is the binding energy between the acceptor and free exciton, the E^{A^0X} is estimated to be 12.6 meV which is equal to thermal energy at 145.4 K, which implies that the bound exciton will be completely ionized from the neutral acceptor when the temperature is above 145.4 K, in agreement with the temperature-dependent PL spectra shown in Fig. 6. The fast reduction in the emission intensity results from the rapid thermal ionization of acceptor-bound exciton with increasing temperature. The thermally ionized acceptor-bound exciton converts into the free-1LO and broadens the emission peak positioned at 3.311 eV.

The room-temperature (RT) spectrum is a very broad emission line consisting of three emission bands centered at about 3.101, 3.242 and 3.265 eV respectively, as shown in the inset of Fig. 6 by using the Gaussian fitting to the spectrum at 300 K. As we know, the room-temperature (RT) PL of high-purity ZnO is dominated by the free-exciton LO phonon replicas' emission with the maximum located close to E_{FX}–1LO energy [35], which is located at about 3.265 eV. So, the emission band centered at 3.265 eV is ascribed to E_{FX}–1LO. The RT emission band centered at 3.242 eV is evolved from the emission peak at 3.311 (80 K) and is ascribed to radiative electron transition from conduction band to Li_{Zn}–N complex acceptor level (eFA).

The RT emission band centered at 3.101 eV is evolved from the emission band centered at 3.165 eV (80 K), this emission is very close to the RT emission peak at 3.030 eV observed in ZnO:Li [32], it may be ascribed to radiative electron transition from conduction band to intrinsic acceptor (eFA_{un}), such as vacancy Zn (V_{Zn}). Fig. 7 also plots the temperature-dependent peak energy for the 3.165 eV (80 K). By fitting the data using Eq. (3), the relevant acceptor level was calculated to be about 273 meV.

4. Conclusions

The optical properties of lithium and nitrogen doped ZnO films were investigated. The transmittances of the as-grown and annealed films were over 95%. From the excitation intensity-dependent PL and temperature-dependent PL measurements, the low-temperature (80 K) emission bands centered at 3.311, 3.346 and 3.219 eV were assigned to emissions of radiative electron transition from conduction band to Li_{Zn}–N complex acceptor level (eFA), a neutral acceptor-bound exciton (A^0X) and donor–acceptor pair (DAP) recombination, respectively. The optical energy level of Li_{Zn}–N complex acceptor was calculated to be about 126 meV above the valence band by fitting the temperature-dependent photon energies of eFA emission bands.

Acknowledgements

We would like to thank financial support of the program of CAS Hundred Talents, Key Projects of the National Natural Science Foundation of China (Grant No. 60336020 and 50532050) and Outstanding Overseas Chinese Young Scholar Foundation No. 60429403, and the Direct Allocation Grant of Research Grants Committee of Hong Kong, No. DAG04/05.SC24.

References

[1] D.C. Look, R.L. Jones, J.R. Sizelove, N.Y. Garces, N.C. Giles, L.F. Halliburton, Phys. Status Solidi a 195 (2003) 171.
[2] Y.J. Zeng, Z.Z. Ye, W.Z. Xu, D.Y. Li, J.G. Lu, L.P. Zhu, B.H. Zhao, Appl. Phys. Lett. 88 (2006) 062107.
[3] H.W. Liang, Y.M. Lu, D.Z. Shen, Y.C. Liu, J.F. Yan, C.X. Shan, B.H. Li, Z.Z. Zhang, J.Y. Zhang, X.W. Fan, Phys. Status Solidi a 202 (2005) 1060.
[4] A. Tsukazaki, A. Ohtomo, T. Onuma, M. Ohtani, T. Makino, M. Sumiya, K. Ohtani, S.F. Chichibu, S. Fuke, Y. Segawa, H. Ohno, H. Koinuma, M. Kawasaki, Nat. Mater. 4 (2005) 42.
[5] D.C. Look, D.C. Reynolds, C.W. Litton, R.L. Jones, D.B. Eason, G. Cantwell, Appl. Phys. Lett. 81 (2002) 1830.
[6] D.K. Hwang, H.S. Kim, J.H. Lim, J.Y. Oh, J.H. Yang, S.J. Park, K.K. Kim, D.C. Look, Y.S. Park, Appl. Phys. Lett. 86 (2005) 151917.
[7] K.K. Kim, H.S. Kim, D.K. Hwang, J.H. Lim, S.J. Park, Appl. Phys. Lett. 83 (2003) 63.
[8] Z.Q. Chen, A. Kawasuso, Y. Xu, H. Naramoto, X.L. Yuan, T. Sekiguchi, R. Suzuki, T. Ohdaira, J. Appl. Phys. 97 (2005) 013528.
[9] P. Wang, N. Chen, Z.G. Yin, Appl. Phys. Lett. 88 (2006) 152102.
[10] Y.R. Ryu, T.S. Lee, H.W. White, Appl. Phys. Lett. 83 (2003) 87.
[11] D.C. Look, G.M. Renlund, R.H. Burgener II, J.R. Sizelove, Appl. Phys. Lett. 85 (2004) 5269.
[12] V. Vaithianathan, B.T. Lee, S.S. Kim, Appl. Phys. Lett. 86 (2005) 062101.
[13] F.X. Xiu, Z. Yang, L.J. Mandalapu, D.T. Zhao, J.L. Liu, W.P. Beyermann, Appl. Phys. Lett. 87 (2005) 152101.
[14] J.G. Lu, Z.Z. Ye, F. Zhuge, Y.J. Zeng, B.H. Zhao, L.P. Zhu, Appl. Phys. Lett. 85 (2004) 3134.
[15] M. Joseph, H. Tabata, T. Kawai, Japan. J. Appl. Phys. 80 (1996) 787.
[16] C.H. Park, S.B. Zhang, S.-H. Wei, Phys. Rev. B 66 (2002) 073202.
[17] M.G. Wardle, J.P. Goss, P.R. Briddon, Phys. Rev. B 71 (2005) 155205.
[18] X.H. Wang, B. Yao, Z.P. Wei, D.Z. Sheng, Z.Z. Zhang, B.H. Li, Y.M. Lu, D.X. Zhao, J.Y. Zhang, X.W. Fan, L.X. Guan, C.X. Cong, J. Phys. D: Appl. Phys. 39 (2006) 4568.
[19] J.G. Lu, Y.Z. Zhang, Z.Z. Ye, L.P. Zhu, L. Wang, B.H. Zhao, Appl. Phys. Lett. 88 (2006) 222114.
[20] T.M. Barnes, K. Olson, C.A. Wolden, Appl. Phys. Lett. 86 (2005) 112112.
[21] C. Suryanarayana, M.G. Norton, X-ray Diffraction: A Practical Approach, Plenum, New York, 1998, p. 263.
[22] N. Ashkenov, B.N. Mbenkum, C. Bundesmann, V. Riede, M. Lorenz, D. Spemann, E.M. Kaidashev, A. Kasic, M. Schubert, M. Grundmann, G. Wagner, H. Neumann, V. Darakchieva, H. Arwin, B. Monemar, J. Appl. Phys. 93 (2003) 126.
[23] J.-G. Lu, Z.-Z. Ye, L. Wang, B.-H. Zhao, J.-Y. Huang, Chin. Phys. Lett. 19 (2002) 1494.
[24] D.L. Dexter, Proceedings of Atlantic City Photoconductivity Conference, Wiley, New York, 1954, pp. 155–183.
[25] J.E. Bardeen, F.J. Blatt, L.H. Hall, Proceedings of Atlantic City Photoconductivity Conference, Wiley, New York, 1954, pp. 146–153.
[26] J.I. Pankove, Optical Processes in Semiconductors, Dover, New York, 1971.
[27] D.G. Zhao, S.J. Xu, M.H. Xie, S.Y. Tong, H. Yang, Appl. Phys. Lett. 83 (2003) 677.
[28] M.-S. Oh, S.-H. Kim, T.-Y. Seong, Appl. Phys. Lett. 87 (2005) 122103.
[29] K. Tamura, T. Makino, A. Tsukazaki, M. Sumiya, S. Fuke, T. Furumochi, M. Lippmaa, C.H. Chia, Y. Segwa, H. Koinuma, M. Kawasaki, Solid State Commun. 127 (2003) 265.
[30] B.K. Meyer, H. Alves, D.M. Hofmann, W. Kriegseis, D. Forster, F. Bertram, J. Christen, A. Hoffmann, M. Strabburg, M. Dworzak, U. Haboeck, A.V. Rodina, Phys. Status Solidi b 241 (2004) 231.
[31] F.X. Xiu, Z. Yang, L.J. Mandalapu, D.T. Zhao, J.L. Liu, Appl. Phys. Lett. 87 (2005) 252102.
[32] L.L. Chen, H.P. He, Z.Z. Ye, Y.J. Zeng, J.G. Lu, B.H. Zhao, L.P. Zhu, Chem. Phys. Lett. 420 (2006) 358.
[33] L.J. Wang, N.C. Giles, J. Appl. Phys. 94 (2003) 973.
[34] R.E. Halstedt, M. Aven, Phys. Rev. Lett. 14 (1965) 64.
[35] W. Shan, W. Walukiewicz, J.W. Agerlll, K.M. Yu, H.B. Yuan, H.P. Xin, G. Cantwell, J.J. Song, Appl. Phys. Lett. 86 (2005) 191911.